A JOINT ANALYSIS OF HIGH-ENERGY NEUTRONS AND NEUTRON-DECAY PROTONS FROM A FLARE

L. G. KOCHAROV, J. TORSTI and R. VAINIO
Space Research Laboratory, University of Turku, SF-20520 Turku, Finland
G. A. KOVALTSOV and I. G. USOSKIN
A.F. Ioffe Physical-Technical Institute, St. Petersburg 194021, Russia

(Received 11 April, 1996; in final form 19 July, 1996)

Abstract. A joint analysis of neutron monitor and GOES data is performed to study the production of high-energy neutrons at the Sun. The main objects of the research are the spectrum of >50 MeV neutrons and a possible spectrum of primary (interacting) protons which produced those neutrons during the major 1990 May 24 solar flare. Different possible scenarios of the neutron production are presented. The high magnitude of the 1990 May 24 neutron event provided an opportunity to detect neutron decay protons of higher energies than ever before. We compare predictions of the proposed models of neutron production with the observations of protons on board GOES 6 and 7. It is shown that the 'precursor' in high-energy GOES channels observed during 20:55 – 21:09 UT can be naturally explained as originating from decay of neutrons in the interplanetary medium. The ratio of counting rates observed in different GOES channels can ensure the selection of the model parameters.

The set of experimental data can be explained in the framework of a scenario which assumes the existence of two components of interacting protons in the flare. A hard spectrum component (the first component) generates neutrons during a short time while the interaction of the second (soft spectrum) component lasts longer. Alternative scenarios are found to be of lesser likelihood. The intensity – time profile of neutron – decay protons as predicted in the framework of the two-component exponential model of neutron production (Kocharov *et al.*, 1994a) is in an agreement with the proton profiles observed on board GOES. We compare the deduced characteristics of interacting high-energy protons with the characteristics of protons escaping into the interplanetary medium. It is shown that, in the 100 – 1000 MeV range, the spectrum of the second component of interacting protons was close to the spectrum of the prompt component of interplanetary protons. However, it is most likely that, at ~300 MeV, the interacting proton spectrum was slightly softer than the spectrum of interplanetary protons. An analysis of gamma-ray emission is required to deduce the spectrum of interacting protons below 100 MeV and above 1 GeV.

1. Introduction

The neutron monitor network is able to detect a solar neutron event. However, it has only a limited capability for a study of the neutron energy spectrum. On the other hand, measurements of spectra of neutron decay protons on board satellites are possible (Evenson *et al.*, 1983, 1990; Evenson, Meyer, and Pyle, 1983; Evenson, Kroeger, and Meyer, 1985). This provides a capability to deduce the spectrum of solar neutrons more exactly. However, for such an approach, it is necessary, firstly, to ensure that the studied proton increase is of the neutron decay nature. What can show whether it is true or not is the observation of the neutrons from the same flare (e.g., Zhang, 1995). Thus, a joint analysis of neutron and proton data is necessary.

Solar Physics **169:** 181–207, 1996.

We perform such an analysis for the 1990 May 24 flare, which was a source of the most powerful neutron event known so far. This is the first time that the analysis is possible for neutrons with some hundreds of MeV energy.

The 1990 May 24 flare has been observed in many high-energy bands and this provided a great deal of information on high-energy particles (Pyle, Shea, and Smart, 1991; Shea, Smart, and Pyle, 1991; Pelaez *et al.*, 1992; Debrunner, Lockwood, and Ryan, 1993; Talon *et al.*, 1993; Terekhov *et al.*, 1993; Kocharov *et al.*, 1993; Kovaltsov, Efimov, and Kocharov, 1993; Kovaltsov *et al.*, 1994; Kocharov *et al.*, 1994a). In particular the flare was a source of high-energy nucleons detected by the neutron monitor network. The 1990 May 24 increase of the neutron monitor counting rate had two distinct peaks. The characteristics of the second increase (at ≈21:11 UT) were normal for a solar proton event. The first increase (at ≈20:51 UT) of short duration was detected only by monitors on the day side of the Earth, and this increase strongly depended on the air mass along the line of sight to the Sun. These circumstances allowed Shea, Smart, and Pyle (1991) to ascribe the first increase to the arrival of solar neutrons. The neutron origin of this increase was proved by Kovaltsov, Efimov, and Kocharov (1993), who noted that the response of neutron monitors to solar neutrons does not follow a simple exponential dependence on the air mass along the line of sight to the Sun because of the contribution of neutrons scattered through large angles. Neglect of this fact might be responsible for misinterpretation of the event.

A part of the solar neutrons decays when moving from the Sun, produces secondary protons. Those protons, if they have been produced near the Earth-connected magnetic line, can be detected before the onset of a major proton event. Three such neutron-decay proton events (21 June, 1980, 3 June, 1982, 25 April, 1984) were detected earlier on board the ISEE-3 spacecraft (Evenson *et al.*, 1990). These neutron-decay proton events were connected with the solar neutron events detected on board the SMM satellite, as well as by ground-based neutron monitors (Chupp, 1990). Since the neutron event of 1990 May 24 was the strongest of those known so far, one can expect neutron-decay protons to be detected for this event as well.

In our previous study (Kocharov *et al.*, 1994a), we examined the properties of the 1990 May 24 flare source region on the basis of an integrated analysis of gamma-ray, high-energy neutron, optical, and microwave data. On the other hand, the major proton event has been studied recently by Torsti *et al.* (1996). We extend these studies with an analysis of possible spectra of interacting high energy ($E > 100$ MeV) protons at the Sun (Sections 4 and 6) and neutron decay protons (Section 5). The onset of the major proton event was clearly seen in the intensity–time profile of the GOES proton channels. We determined the fact that some weak increase was clearly seen in the high-energy channels before the onset of the major proton event. Neutron-decay protons should produce such a 'precursor'. Inasmuch as, for this flare, high-energy neutrons were measured by neutron monitors, and interplanetary proton transport parameters are known (Torsti *et al.*, 1996), one has

a good chance to use this 'precursor' for a verification of the parameters of neutron injection from the Sun.

2. Observations

The flare of 1990 May 24 (X9.3/1B; N33 W78) occurred during 20:46 - 21:45 UT in the active region NOAA 6063. Optical and microwave emissions of the flare were discussed extensively by Kocharov *et al.* (1994a, 1996). Two sources of the emissions were revealed. High-frequency microwave (10 GHz) and optical (Hα and HeD3) emissions were produced in a source of size $\approx 2 \times 10^9$ cm, while low-frequency microwave emission (1 GHz) came from a source of size $\approx 2 \times 10^{10}$ cm. Both sources were equally powerful in the microwave band. This resulted in a flat spectrum of the emission at the maximum of the burst (Lee, Gary, and Zirin, 1994). An exponential decay of 1 GHz emission started one minute after the burst maximum, had an e-folding time $\approx$ 220 s, and lasted about 17 min.

Radiation in the 2.2 MeV gamma-ray line was detected during the flare by the PHEBUS instrument on board the GRANAT observatory (Terekhov *et al.*, 1993). The decaying 2.2 MeV line photon flux was detected during more than 8 min after the 4 – 6 MeV intensity maximum. The e-folding time of the 2.2 MeV emission gradually increased from $\approx$ 180 s up to $\approx$ 360 s during this time (the mean value of the e-folding time was 260 s for this time interval). The 4 – 6 MeV intensity maximum coincided with the second peak in high-energy (57.5 – 110 MeV) gamma-ray emission (see Figure 1). Talon *et al.* (1993) emphasized a hardening of the high-energy gamma-ray emission spectrum at the onset of the second peak (20:48:27 UT) and concluded that 'hardening of the spectrum above 50 MeV during the second peak strongly suggested that meson decay gamma-ray radiation is dominant' (see also Vilmer, 1994; and Trottet, 1994). Terekhov *et al.* (1993) determined the fact that the second peak in 65 – 124 MeV band coincided with the maximum of 4 – 6 MeV radiation, which gives additional support to the nuclear dominant explanation of the peak (see also Figure 9 by Talon *et al.*, 1993). On the other hand, it was noted by Terekhov *et al.* (1993) that the counting rate in the PHEBUS 57.5 – 110 MeV-channel did not decay down to the background level, as was observed at lower energies. This temporal behaviour was explained by the PHEBUS team to be a result of a contamination of the 57.5 – 110 MeV channel by solar neutrons (Talon *et al.*, 1993; Terekhov *et al.*, 1993). Figure 1 illustrates this interpretation. Solar neutrons are regarded as a source of the excess of the 57.5 – 110 MeV channel counting rate observed after 20:50 UT.

Keeping in mind that the 2.2 MeV gamma-ray line emission had an extremely long decay time, which is a signature of long-lasting interaction of accelerated protons with solar matter (Kocharov *et al.*, 1994a), we approximate the time profile of high-energy gamma-ray emission with two exponents:

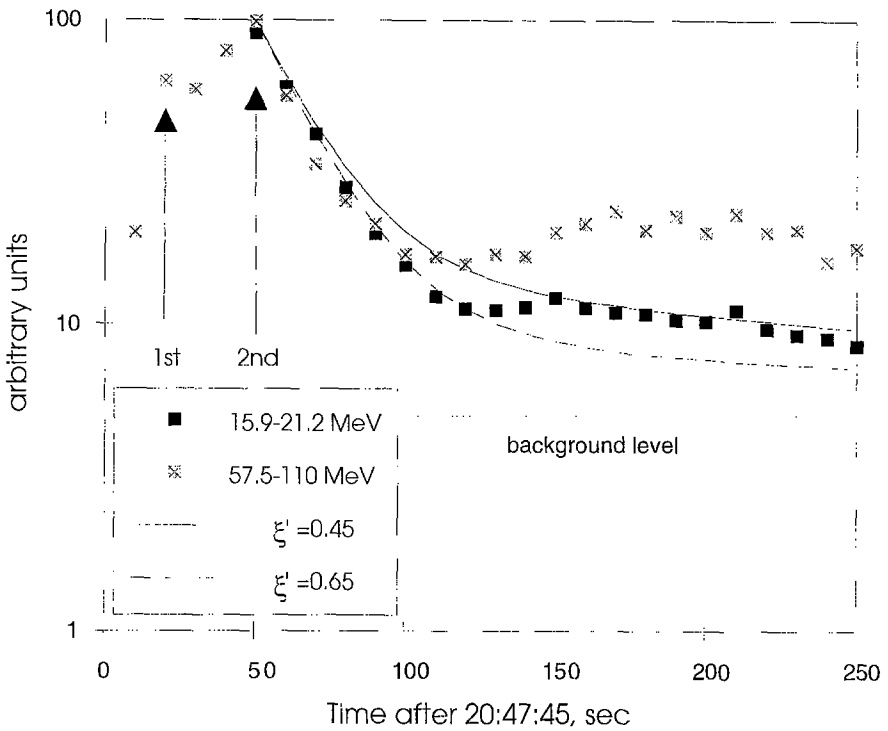

Figure 1. The temporal evolution of the 1990 May 24 gamma-ray/neutron event as observed by the PHEBUS detectors in two energy bands, 15.9 - 21.2 and 57.5 - 110 MeV (Talon *et al.*, 1993). Arrows show the two peaks discussed. Curves illustrate the approximation of high-energy gamma-ray flux according to Equation (1) for different values of the parameter ξ', $T_f = 20$ s, $T_s = 260$ s.

$$I(t) = \Gamma \Sigma \left[\frac{\xi'}{T_f} \exp\left(-\frac{t}{T_f} \right) + \frac{1 - \xi'}{T_s} \exp\left(-\frac{t}{T_s} \right) \right] . \tag{1}$$

where e-folding times for the first (f) and the second (s) components of the emission, T_f and T_s, are taken from the observations of high-energy and 2.2 MeV gamma-ray emissions respectively; the 'zero' time is 20:48:30 UT. The parameter ξ', which is the contribution of the first component of the emission to the total fluence, should be adjusted to fit the observed time profile. One can see from Figure 1, that it is most likely that $\xi' = 0.5 - 0.6$. This indicates that both the components (almost) equally contribute to the high-energy emission. In what follows, we use the designations f and s for those interacting particles which produce gamma-ray emissions and neutrons at the Sun, as well. The >300 MeV protons are considered to be a natural source of high-energy gamma-ray emission observed after 20:48:30 UT. As an alternative, it might be proposed that electron bremsstrahlung was responsible for both peaks shown in Figure 1. However, one can see from Figure 15 by Pelaez *et al.* (1992) and Figure 10 by Talon *et al.* (1993) that the 'electron-dominated' explanation of the second sub-peak would implicate simultaneous hardening of the

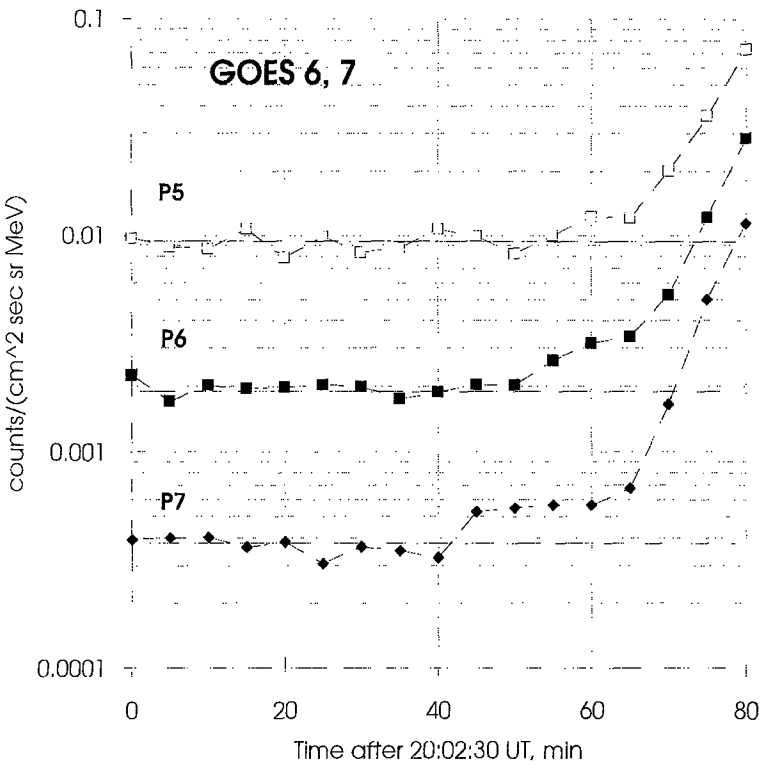

Figure 2. The 5-min-average uncorrected counting rate observed on board GOES 6 and 7 in three proton channels (averaged over the two satellites). A 'precursor' is seen before the onset of the major proton event. The background levels are shown by solid lines.

electron spectrum for energies above 50 MeV and softening of the spectrum in the 0.8–15 MeV energy band. We cannot exclude such a complicated behaviour of the electron spectrum, but it seems to be less probable than the 'pion dominated' scenario by Talon *et al.* (1993).

The flare of 1990 May 24 was a source of a strong ground level event (GLE). The first increase detected by neutron monitors (20:49–21:03 UT) was caused by the arrival of high-energy solar neutrons. The high magnitude of the 1990 May 24 neutron event provided an extraordinary chance to study properties of neutron production at the Sun. Climax neutron monitor data for the neutron event were of the highest significance among the neutron monitors as well as of good, one-minute, time resolution. Thus these data are the most suitable for the analysis. In the present paper, we make use of records of neutron monitor counting rate taken from the GLE Data Base (WDC-A). For the study of neutron decay protons, we employ data from the GOES 6 and 7 satellites on detection of protons at the Earth's orbit (CD GOES, 1992).

In Figure 2 we show the mean of GOES 6 and GOES 7 5-min averaged uncorrected counting rates. Background levels as obtained by averaging over the 19:40–

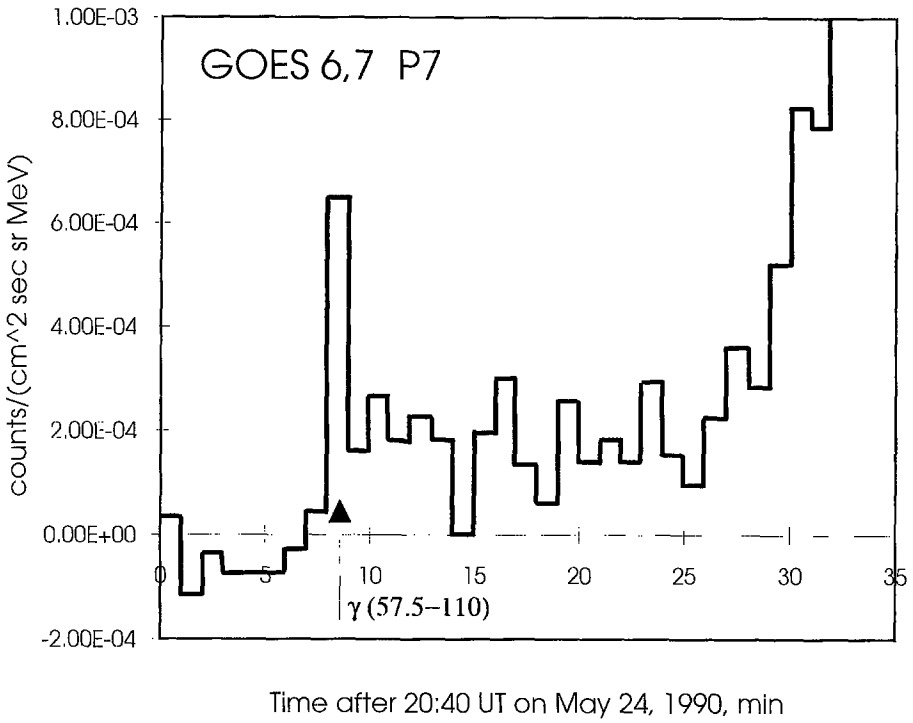

Figure 3. The 1-min-average uncorrected counting rate observed in the P7 channel on board GOES 6 and 7 (averaged over the two satellites). The background level is subtracted. The arrow illustrates the time of the maximum of the 57.5 – 110 MeV gamma-ray emission as observed by PHEBUS/GRANAT detectors.

20:40 UT interval are shown by solid lines. A 'precursor' is clearly seen in P7 and P6 channels before the major proton event. A less distinct 'precursor' may be seen in the P5 channel after 21:00 UT. It is seen from minute-averaged GOES data (Figure 3) that the onset of the precursor in the P7 channel coincided with the sharp maximum of the 57.5 – 100 MeV gamma-ray emission as observed by the GRANAT/PHEBUS detectors (Figure 1). The sharp pulse was seen in the P7 channel during the first minute (20:48 – 20:49 UT) only. The height of the pulse exceeded the 10σ level. It is known that a charged-particle detector has some sensitivity to gamma-ray emission as well (e.g., Kocharov *et al.*, 1994b). No other emission in this energy band (110 – 500 MeV) but gamma-rays can arrive during the first minute. Furthermore, protons, whenever being injected from the Sun, cannot produce one-minute pulses because of the velocity dispersion. For these reasons, one has to conclude that high-energy gamma-rays are the main source of the first portion of the P7 channel 'precursor'. The nature of the second portion of the precursor (20:55 – 21:09 UT) will be studied in Section 5.

3. The Model

3.1. Injection of Neutrons

A ground-based neutron monitor can effectively detect solar neutrons with energy >300 MeV. It is usual for a study of solar neutron events to employ a model of neutron injection from the Sun, with some spectral and temporal parameters, to calculate an expected response of neutron monitors for those neutrons and to obtain values of the parameters on the basis of a comparison of the expected response with the actual one. In a limited energy band (namely, 100 MeV – 1 GeV), different approximations of neutron spectra can be adopted. For instance, Chupp *et al.* (1987) made use of, among others, exponential neutron spectra. More often, a power-law spectrum with an upper cutoff is employed (Chupp *et al.*, 1987; Debrunner, Lockwood, and Ryan, 1993). In our previous paper (Kocharov *et al.*, 1994a), we considered neutron injection from the Sun, proposing the neutron injection spectrum to be exponential in energy. As the next step in the study, we start directly from the spectrum of primary protons producing neutrons in nuclear interactions with solar matter. A power-law proton spectrum of interacting protons is employed, $N(E) \sim E^{-S}$, with cutoff energy c. Thus we use for the analysis a solar neutron injection spectrum, $F(S) \equiv F(E, S, c)$ (neutron MeV^{-1}), which is the spectrum of neutrons produced by protons with a power-law spectrum in energy. (The neutron spectrum itself is not a power-law one.) The energy spectrum of neutrons produced by those protons in the solar atmosphere has been calculated for the isotropic thick-target model by means of the Monte-Carlo technique described by Gueglenko *et al.* (1990). Throughout the present paper, this neutron spectrum is identified as the $F(S)$ spectrum. The $F(S)$ spectrum is normalized per one interacting proton with energy above 600 MeV. Usually, the energy of 30 MeV is used as the normalisation energy when dealing with interacting proton spectra. In the present paper, we make use of 600 MeV as the normalisation energy for the interacting proton spectrum, because such protons effectively produce high-energy neutrons detected by neutron monitors. The $F(S)$ spectrum as well as the exponential neutron spectrum adopted by Kocharov *et al.* (1994a) is a theoretical tool for the analysis. Only a comparison of calculations with experimental data may show which neutron spectrum is closer to the actual spectrum of neutrons produced during the flare. However, the convenience of $F(S)$ is that it shows explicitly the slope of the interacting proton spectrum (in the corresponding energy band). In our calculations, the helium abundance He/p = 0.07 is employed (similar to Hua and Lingenfelter, 1987). A possible impact of higher values of the He/p-ratio has been studied additionally.

The employed model of neutron injection during the flare is based on the multi-wavelength study, including gamma-ray, microwave, and optical emissions (Kocharov *et al.*, 1994a, 1996, and Section 2 of the present paper). In the framework of this

model, the function of neutron injection towards the Earth (neutron $sr^{-1} s^{-1} MeV^{-1}$) is taken as

$$I_{\odot}(E,t) = \frac{N_0(>600\ \mathrm{MeV})}{4\pi} \left[\frac{\xi}{T_f} F(E,S_f,\epsilon_f) \exp\left(-\frac{t}{T_f}\right) + \frac{1-\xi}{T_s} F(E,S_s,\epsilon_s) \exp\left(-\frac{t}{T_s}\right)\right] . \quad (2)$$

where $N_0(>600$ MeV) is the total number of >600 MeV protons interacting at the Sun (in the case of isotropic neutron production); ξ is the portion of the first component protons in the total proton number $N_0(>600$ MeV); $S_{f(s)}$ and $T_{f(s)}$ denote proton spectral index and injection decay time of the first (f) or second (s) component. In Equation (2), the moment $t = 0$ corresponds to 20:48:30 UT. Values of the decay time of the neutron injection are taken as $T_f = 20$ s and $T_s = 260$ s. Note that a 30% variation of these values would not lead to any essential change in the results of the analysis.

Simultaneously with high-energy neutrons, π^0-mesons are produced which is the most likely source of 57.5–110 MeV emission observed after 20:48:30 UT. Ultra-relativistic electrons may also contribute to this emission. However this cannot affect the conclusion that the time profile of high-energy gamma-ray emission is the best empirical basis for a high-energy neutron production model, since high-energy gamma-rays are a signature of particles accelerated to the highest energies, anyway. Thus, in a view of Figure 1, it is most likely that $\xi = \xi' = 0.5–0.6$. This circumstance was actually the initial point of Kocharov *et al.* (1994a). To perform an alternative study, we analyse all values of the parameter $\xi \in [0, 1]$ in the present paper.

3.2. Neutron Decay Protons

Models of the propagation of protons produced by decay of solar flare neutrons were developed by Kurganov and Ostryakov (1989, 1992) and by Ruffolo (1991). These models treat the deposition, pitch-angle scattering, adiabatic focusing, and adiabatic deceleration of neutron-decay protons. We take these effects into account. However, we use another calculation technique than the one used in the papers above. In the present study, the propagation of secondary protons is traced by means of Monte-Carlo simulations. This technique is similar to that applied to escaping (interplanetary) protons and relativistic electrons in our recent study of the major solar cosmic-ray event of 1990 May 24 (Torsti *et al.*, 1996) where two components (*prompt* and *delayed*) of interplanetary protons have been discussed. In contrast to the prompt component of interplanetary protons, neutron decay protons are injected not only at the foot of the interplanetary magnetic field line connected to the Earth but along the line as well. That is why the injection function of secondary protons should be taken as

$$Q(z,\mu,t) \equiv \frac{\mathrm{d}^4 N_{n\to p}}{\mathrm{d}z\,\mathrm{d}\mu\,\mathrm{d}t\,\mathrm{d}S_\odot} = I\{\alpha(z),t'\}\frac{B_\odot}{\gamma\tau V B(z) r(z)^2}\times$$

$$\times \exp\left\{-\frac{r(z)}{\gamma\tau V}\right\}\delta\{\mu-\cos\psi(z)\}\ . \tag{3}$$

where $Q(z,\mu,t)$ is the rate of neutron-decay proton production per unit of the magnetic line length, z, and per unit of the magnetic tube cross-section at the Earth's orbit, $S_\odot$ (i.e., we consider the production at any point along the magnetic line as calculated per unit of the magnetic tube cross-section near the Earth); $\alpha(z)$ is the angle between the normal to the solar surface at the flare site and the direction to the point where the length of the magnetic line is equal to z (i.e., $\alpha(z)$ is the zenith angle as seen from the flare site); $I\{\alpha,t'\}$ is the intensity of neutron emission from the Sun (neutron sr^{-1} s^{-1}) in a certain zenith angle, α, at time $t' = t - r(z)/V$; $r(z)$ is the radial distance to the Sun; $\psi(z)$ is the inclination of the interplanetary magnetic field line (see, e.g., Figure 8 of Torsti *et al.*, 1996); B is the magnetic field strength; V, γ, and τ refer to the velocity, Lorentz-factor and decay time of a neutron, respectively. It is essential that the use of the mean free path for the neutron-decay protons be similar to that for the *prompt* component of escaping protons (see Torsti *et al.*, 1996), i.e., the mean free path of neutron decay protons is not an adjusting parameter. The total number of traced secondary protons was $\approx 2\times 10^6$ in each set of calculations.

In our calculation we made use of the intensity of neutron emission towards the Earth, $I_\odot$, deduced from neutron monitor data (see Equation (2)). In order to calculate the flux of neutron-decay protons, one should adopt some angular distribution of neutron emission from the Sun, since those protons are produced at any point along the Earth, connected magnetic field line. The magnetic field line connected at the Earth's was seen from the flare site at zenith angles $\alpha = 40°$–$90°$. In a general case, one may expect that the intensity $I\{\alpha,t'\}$ increases with α. The actual value of anisotropy of neutron emission depends on the magnetic environment at the flare site. Recently, we considered the angular distribution of neutron emission from the 1991 March 22 solar flare (Kocharov *et al.*, 1995). This flare was found to be similar to the 1990 May 24 flare with respect to optical and microwave emissions. However, the flux of high-energy neutrons as deduced from neutron monitor data for the 1991 March 22 flare was lower, which might be caused by the difference in the two flare locations on the solar disk. In the case of the 1991 March 22 flare, the Earth was seen from the flare site at zenith angle $\alpha_\odot = 33°$, while $\alpha_\odot$ was 80° in the case of 1990 May 24 flare. It was found that a relative neutron brightening, A_Δ, of the 1990 May 24 flare due to this difference in the zenith angle was not large: $1 \le A_\Delta \le 3$. Taking into account this comparison, we consider two possibilities for the angular distribution of solar neutrons: (i) the isotropic neutron emission ($A_\Delta = 1$ along the magnetic field line); (ii) moderate weakening of neutron emission at small α (by factor $A_\Delta = 2$), $I\{\alpha,t'\} = I_\odot/A_\Delta$ at $\alpha < 57°$ (for illustration see Figure 8 by Torsti *et al.*, 1996).

Table I
Best-fit parameters of interacting proton spectra

ξ	S_f	S_s	$\frac{N_0(>600\ \mathrm{MeV})}{10^{30}}$	$\chi^2(13)$
0.00	–	1.6	3.2	10.9
0.10	2.0	2.1	3.4	7.6
0.30	2.9	3.0	4.4	9.9
0.40	3.1	3.6	4.7	12.3
0.50	3.1	4.4	4.5	13.4
0.60	3.2	5.0	4.1	13.3
0.70	3.3	5.5	3.9	12.8
0.90	3.4	6.8	3.4	13.1
0.95	3.5	7.3	3.4	14.6
0.97	3.6	7.4	3.7	22.4
0.40	3.0	Eq. (4)	4.4 ($Y = 0.0$)	15.0
0.44	3.1	Eq. (4)	4.2 ($Y = 1.0$)	13.9
0.48	3.1	Eq. (4)	4.0 ($Y = 2.0$)	13.1
0.50	3.1	Eq. (4)	3.8 ($Y = 3.0$)	12.7

The proton intensities obtained were recalculated to uncorrected GOES counting rates with all the secondary channels taken into account (similar to Torsti *et al.*, 1996).

4. Analysis of Neutron Monitor Data

The analysis was carried out by means of a comparison of the simulated response of the Climax neutron monitor for the 1990 May 24 event with the observed one by a χ^2-test. The comparison was done for 14 one-minute intervals from the start of the counting rate increase at 20:49 UT until the arrival of first relativistic protons at the Earth's orbit at 21:03 UT. We also took into account the fact that there was no significant response of the monitor during 20:48–20:49 UT. We varied the model over 5 parameters: ξ, S_f, S_s, ϵ_f, and ϵ_s. A finite value of the cutoff energy has been found to be essential for the first component only, $\epsilon_f \leq 5$ GeV, otherwise the counting rate of the Climax monitor during the first minute interval (20:48–20:49 UT) must be much higher than the observed one. The results presented in this paper are shown for $\epsilon_f = \epsilon_s = 5$ GeV. Examples of the fits obtained are shown in Figure 4. The best-fit parameters are presented in Table I. In Figure 5 we show the 90% confidence contours in the (S_f, S_s)-plane for different possible values of the parameter ξ. (The 90% confidence corresponds to the value of $\chi^2(13) = 19.8$.)

Two qualitatively different cases can be seen in Figure 5. First, in the range of $\xi \leq 0.46$, it is possible to have equal spectral indices for the components. In this case, both the components may be considered as different portions of a single

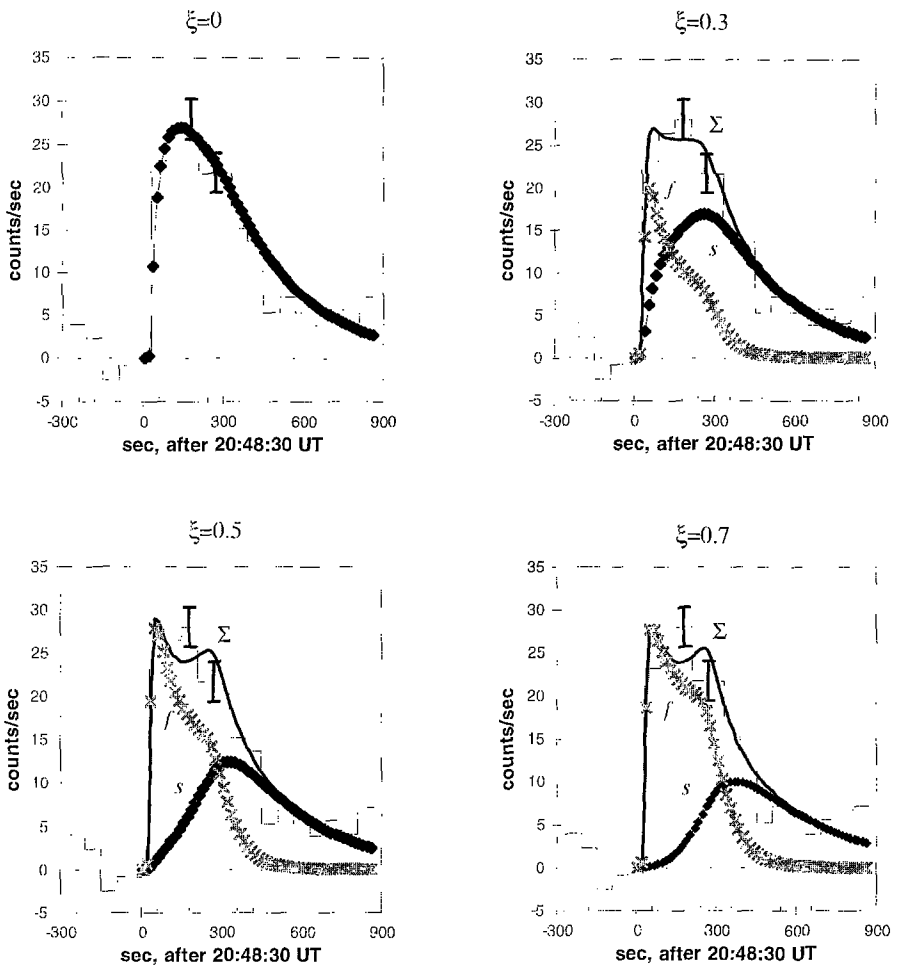

Figure 4. The illustration of fitting to the Climax neutron monitor counting rate at different model parameters (see Table I). Contributions of the first (f) and the second (s) components of solar neutrons into the total calculated counting rate (Σ) are shown. In the case of $\xi = 0$, no impulsive neutron production is proposed. The histogram with error bars represents the observed counting rate.

population of accelerated particles at the flare site (cf., Guglenko *et al.*, 1990). The 90% confidence contour for the case $S_f = S_s$ is shown in Figure 6. It is seen that a possible spectrum of interacting protons is rather hard, $S_f = S_s \leq 3.4$. In contrast, at $\xi > 0.46$, the s-component spectrum is always softer than the spectrum of f-component protons. In particular, the value of S_s could possibly be equal to the spectral index of ≈ 1 GeV interplanetary protons, $S_p = 4.5$ (*prompt* component protons according to Torsti *et al.*, 1996). It is noteworthy that the spectral index of s-component protons becomes close to that of interplanetary particles when the parameter ξ takes its most likely value $\xi = 0.5$ (as discussed in Sections 2 and 3.1). One case of each type has been sampled for more detailed analysis:

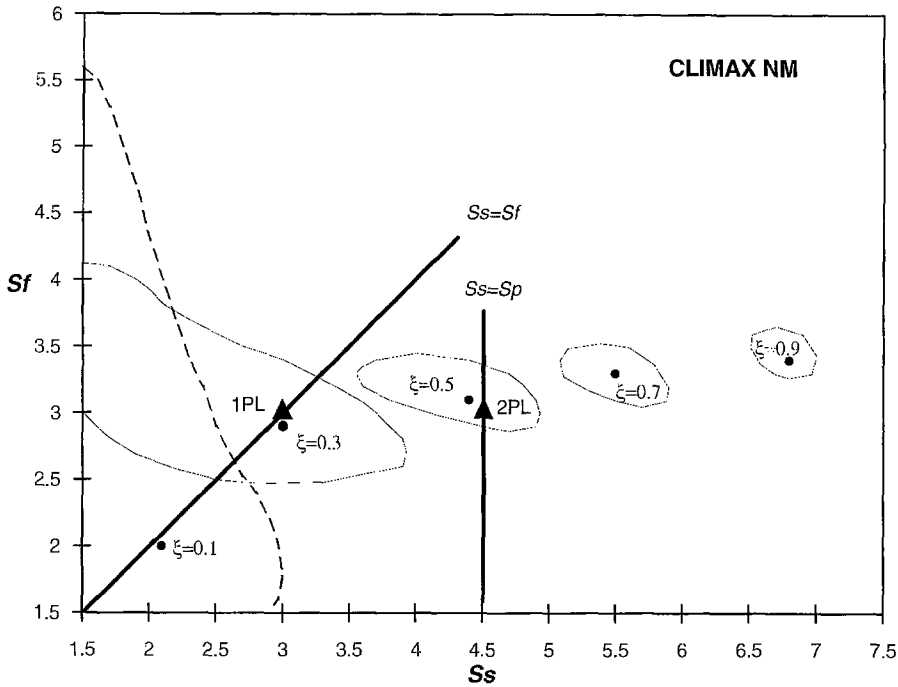

Figure 5. The results of the parameter fitting of the Climax neutron monitor counting rate at different values of the parameter ξ. The contours represents the 90% confidence level in the proton spectral index plane (S_f, S_s). The line $S_s = S_f$ corresponds to the case when the first and second components of interacting protons may be considered as different portions of a single population of interacting particles at the Sun. The $S_s = S_p$ line illustrates the case when the second component spectrum is close to the spectrum of the *prompt* component of interplanetary protons at ≈ 1 GeV. Black triangles marked with 1PL and 2PL show the values of parameters sampled for calculations of neutron decay protons.

(i) $S_f = S_s = 3.0$ at $\xi = 0.3$, and (ii) $S_f = 3.0$, $S_s = 4.5$ at $\xi = 0.5$ (marked with 1PL and 2PL in Table II, respectively). In the next section, we will compare expected fluxes of neutron decay protons for 1PL and 2PL cases with the GOES observations to deduce the actual neutron spectrum in the event. Other possibilities will be discussed as well.

5. Neutron Decay Protons

We compare intensity – time profiles observed in the high-energy GOES channels (P5 – P7) with neutron decay profiles expected for different cases listed in Table II. All the observed counting rates are averaged over the two GOES satellites to get better statistics. Background levels are subtracted. Figure 7 shows calculated and observed profiles in the P6 (84 – 200 MeV) channel. As was discussed in Section 2, the excess of the P7 (110 – 500 MeV) channel counting rate observed

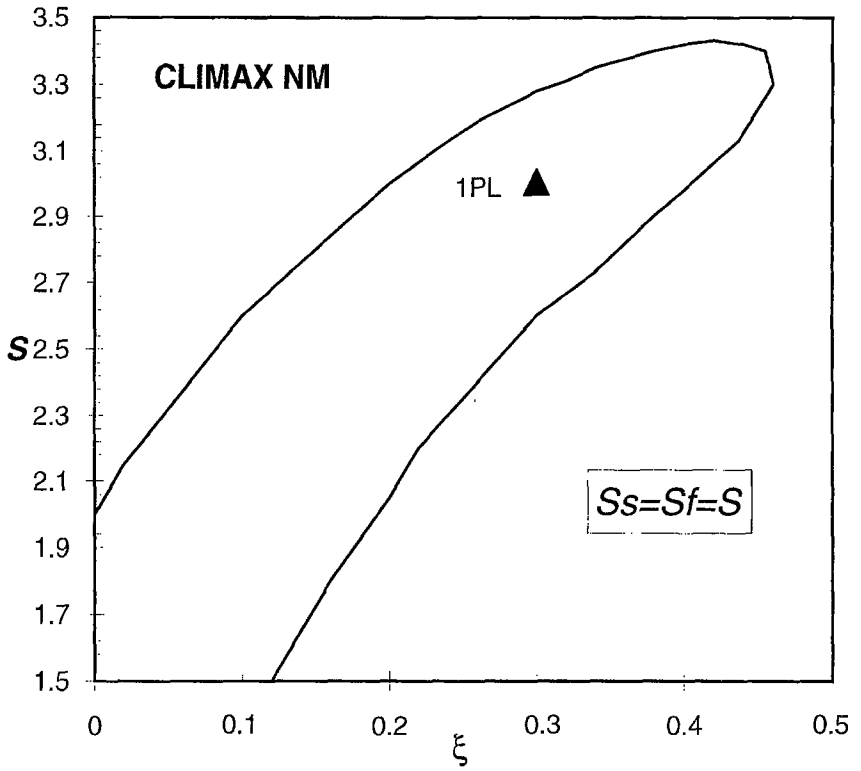

Figure 6. The results of the parameter fitting of the Climax neutron monitor counting rate. The contour represents the 90% confidence level in the proton spectral index vs the parameter ξ plane. The contour is obtained with the constraint $S_s = S_f = S$. In this case, the first and the second components of the interacting protons may be considered as different portions of a single population of interacting particles at the Sun. The triangle marked '1PL' shows the values of parameters sampled for calculations of neutron-decay protons.

Table II

Parameters for calculation of neutron-decay protons

ξ	S_f	S_s	S_3	$\frac{N_0(>600\ \text{MeV})}{10^{30}}$	A_Δ	$\frac{N^{(3)}(>600\ \text{MeV})}{10^{30}}$	ID
0.30	3.0	3.0	–	4.4	1.0	0.0	1PL
0.50	3.0	4.5	-	4.5	2.0	0.0	2PL
0.40	3.0	Eq. (4)	-	4.4	1.0	0.0	BPL
0.30	3.0	3.0		4.4	2.0	0.0	1PLA
0.40	3.0	3.0	4.5	4.0	2.0	1.0	3PLA
0.55	$E_f =$ 310 MeV	$E_s =$ 80 MeV		[a]	2.0	-	EXP[a]

[a] Only in the EXP case, $\xi = N_f^{(\text{neutron})}(>300\ \text{MeV})/N_0^{(\text{neutron})}(>300\ \text{MeV})$, $N_0^{\text{neutron}}(>300\,\text{MeV} = 1.0 \times 10^{30}$ (according to Table I by Kocharov *et al.*, 1994a, for $T_s = 260$ s).

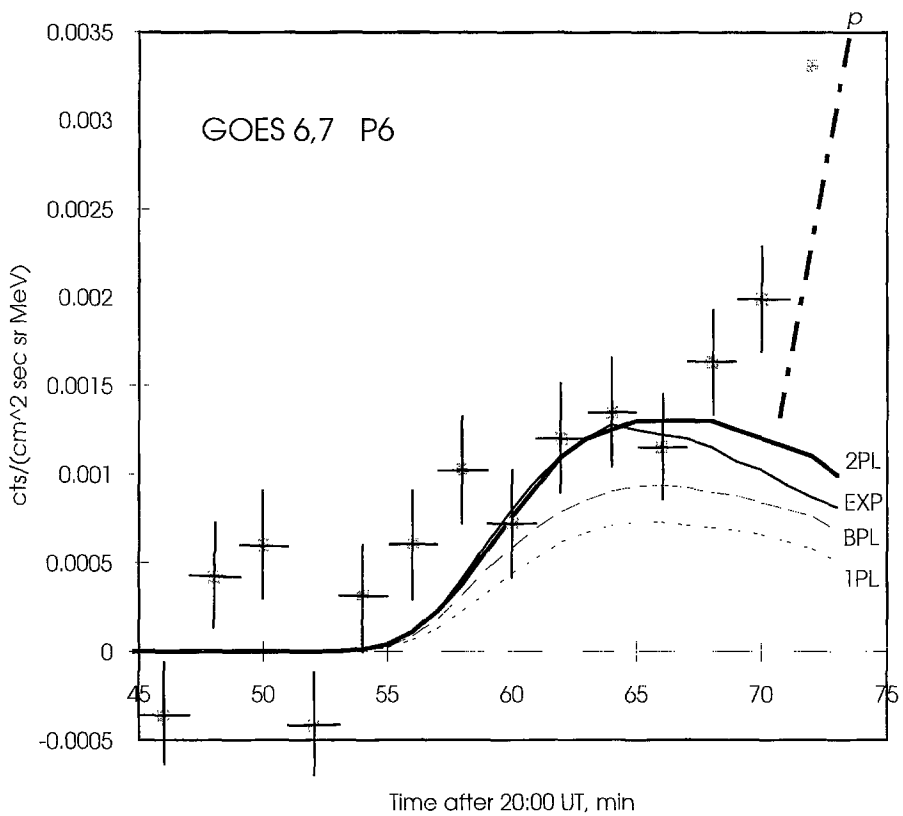

Figure 7. The observed (points) and calculated (curves) counting rates of the GOES P6 channel during the time when the 'precursor' was observed. The intensity–time profiles of neutron-decay protons have been calculated for the cases listed in Table II. The observed counting rate is averaged over the two GOES satellites with the background subtracted. The error bars illustrate the standard deviation of the counting rate as observed on board GOES 6 and 7 during 19:40–20:40 UT on May 24, 1990. The EXP case corresponds to the exponential model by Kocharov *et al.* (1994a). The BPL case is discussed in Section 6. The dash-dotted line marked with *p* shows the onset of the major proton event.

during 20:48–20:49 UT was caused by high-energy gamma-rays. For this reason, we suppose the time profile of gamma-ray contamination in the P7-channel to be equal to that given by Equation (1) at $T_s = 260$ s, $T_f = 18$ s, and $\xi' = 0.47$. This time profile has been normalized to the observed P7-channel counting rate during 20:48–20:49 UT and subtracted from the actual P7-channel counting rate. The resulting intensity–time profile is shown in Figure 8 along with calculated profiles of neutron-decay protons.

Different possible parameters of neutron injection have been studied. The calculated shape of the intensity–time profile of neutron-decay protons is not very sensitive to the choice of the neutron injection scenario (spectrum). This is so because we consider only scenarios which fit the neutron monitor counting rate

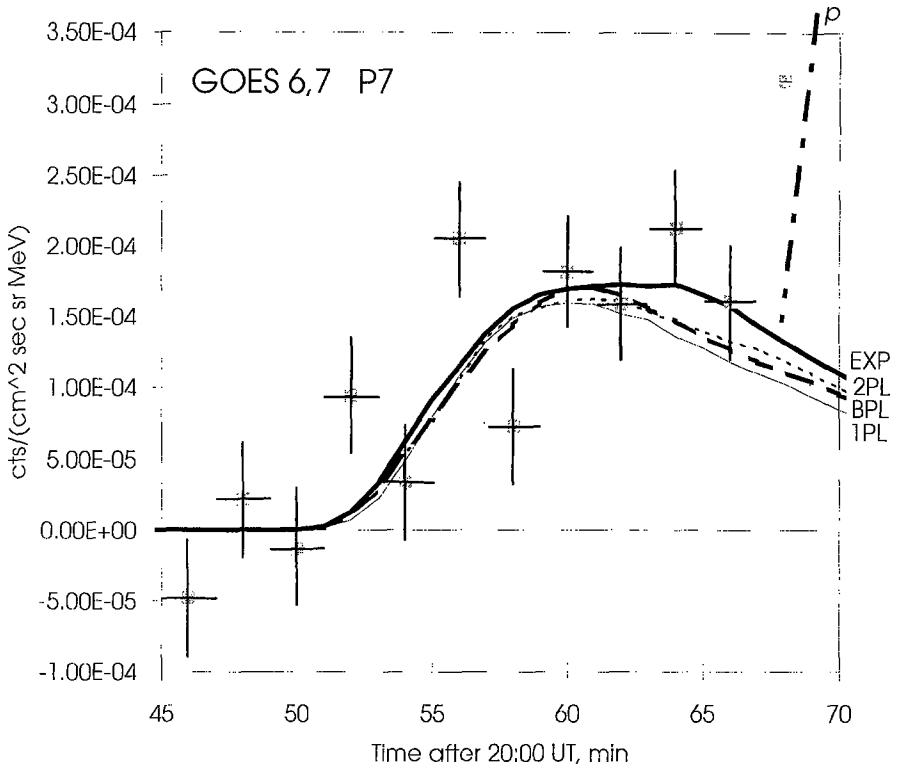

Figure 8. The observed (points) and calculated (curves) counting rates of the GOES P7 channel during the time when the 'precursor' was observed during the 'precursor' observed in the P7-channel. The intensity – time profiles of neutron decay protons have been calculated for the cases listed in Table II. The observed counting rate is averaged over the two GOES satellites with the background and gamma-ray contamination subtracted. The error bars illustrate the standard deviation of the counting rate as observed on board GOES 6 and 7 during 19:40–20:40 UT on May 24, 1990. The BPL case is discussed in Section 6. The dash-dotted line marked with p shows the onset of the major proton event.

actually observed. In contrast, the calculated ratio of the proton counting rates in different GOES channels depends mainly on the neutron injection spectrum. Note that the calculated maximum value of the proton intensity depends on the value of the anisotropy factor A_Δ. However, we have no fitting parameters for the shape of the proton intensity–time profile and for the ratio of the intensities in different energy channels. The maximum value of the intensity may be obtained at $A_\Delta = 1$. In the case of hard neutron spectra, corresponding to $\xi \leq 0.46$, the calculated flux of neutron-decay protons is low. For this reason, the extreme value of $A_\Delta = 1$ is used to get the best possible agreement. For a comparison, Figure 9 shows the results of calculations for hard neutron spectra at $A_\Delta = 2$, as well (see curves 1PL and 1PLA). In the case of a soft spectrum of s-component neutrons ($\xi > 0.46$) we use $A_\Delta = 2$ which corresponds to a moderate limb brightening of the neutron emission.

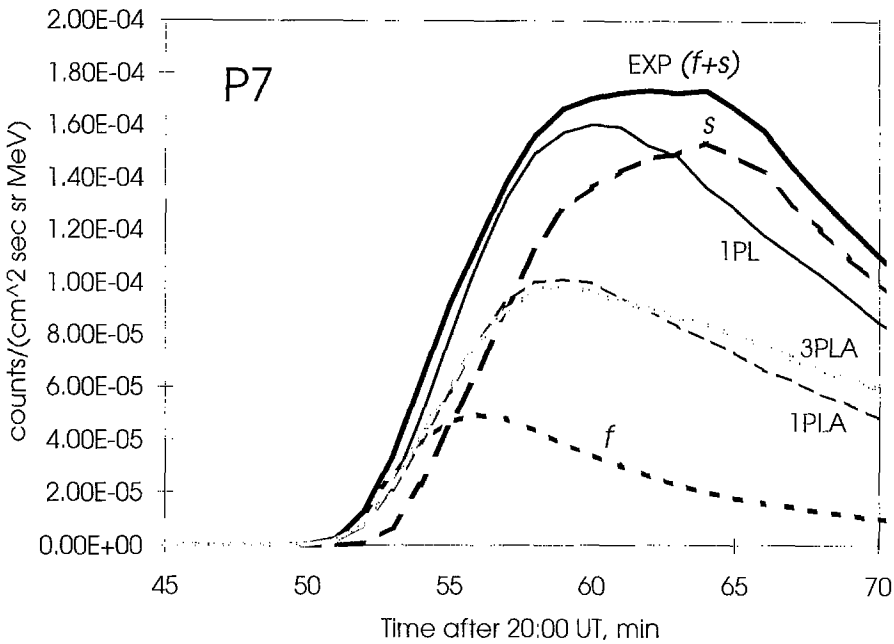

Figure 9. The calculated intensity - time profiles of neutron decay protons expected in the P7-channel for different cases listed in Table II. The dashed curves f and s illustrate partial contributions of the first and second components of neutrons for the EXP case. The 3PLA curve is discussed in Section 7.2.

The 'precursor' observed after 20:55 UT on board GOES can be explained naturally as caused by neutron-decay protons because (i) neutrons from the 1990 May 24 flare were detected by neutron monitors, (ii) the proton intensity – time profile observed during the precursor is consistent with the neutron intensity – time profile observed by the neutron monitor. However, in the case of hard neutron spectra (e.g., case 1PL), the expected maximum flux of neutron-decay protons is lower than the flux observed in the P6 channel (Figure 7). The reason is that all the calculated curves are based on the fitting of the Climax neutron monitor counting rate. This implies that the number of >300 MeV neutrons is about the same for each curve. The GOES channels are available at lower energies. Hence, the GOES counting rates turn out to be sensitive to the slope of the neutron spectra at 100 – 300 MeV. As a result, none of the hard neutron spectra can fit the P6-channel counting rate. Note that an attempt to increase $S_s = S_f$ up to the maximum possible values, 3.3 – 3.4, results in an excess of the counting rate in the P5-channel with only a slight increase in the P6 channel. In contrast, a soft spectrum of s-component neutrons, $F(S = 4.5)$, fits the precursor observed in the P6 and P7 channels very well (see 2PL curves in Figures 7 and 8).

In addition, Figures 7 and 8 show the proton fluxes expected in the frame of the exponential model (Kovaltsov *et al.*, 1994; Kocharov *et al.*, 1994a), which also suggests a soft spectrum of s-component neutrons, $N_S^{\text{neutron}}(E) \sim \exp(-E/E_S)$,

where $E_s = 80$ MeV (marked with EXP in Table II). It is seen that the prediction of the exponential model is in agreement with the GOES observations.

A comparison of the expected and observed fluxes of neutron decay protons is summarised in Figure 10. One 5-min bin in each channel is sampled for this figure. It is seen that the slope of the neutron spectrum between 100 and 500 MeV was close to that of the $F(S = 4.5)$ spectrum (2PL case). In the 1PL case ($F(S = 3.0)$ spectrum), the expected P6-channel counting rate is essentially lower than the observed one (the discrepancy is 3.5σ). At the same time, the slope of the neutron spectrum between 50 and 100 MeV was definitely less than that for the $F(4.5)$-spectrum. In this energy band, the slope was close to that expected in the case of the exponential model. Thus, in the entire 50–500 MeV band, the neutron spectrum may be fitted with an exponent in energy. The calculated neutron spectra are shown in Figure 11. It is seen that, in the 100–500 MeV band, the exponential spectrum of s-component neutrons comes close to the spectrum $F(S = 4.5)$. Of course, the difference between the spectra is large in the range above 500 MeV, but it does not affect the GOES and neutron monitor counting rates expected. In the following sections, we will discuss a possibility to explain the flattening of neutron spectrum below 150 MeV.

6. Interacting Protons versus Interplanetary Protons

When analysing neutrons as detected by neutron monitors, one can extract some information on spectra of primary protons with energy >300 MeV which are responsible for the production of >150 MeV neutrons at the Sun. This is seen from the observations of neutron decay protons in the interplanetary medium that the spectrum of s-component of interacting protons was close to $E^{-4.5}$ in this energy band. It implies that an additional hard f-component of interacting protons (with a spectrum $E^{-3.2\pm0.3}$) is needed to fit the time profile of the neutron monitor counting rate (Figure 5; as an illustration, see also the third frame in Figure 4). Note that the f-component almost does not contribute to the production of those neutron decay protons which can be observed in the GOES P5–P7 channels (Figure 9). It is seen from Figure 5 that the value of the parameter ξ, is close to 0.5 in this case. This means that both components (f and s) contained about the same number of >600 MeV protons.

The total number of >600 MeV protons interacting at the Sun is almost independent of the details of the scenario: $N_0(> 600\,\text{MeV}) = (4 \pm 1) \times 10^{30}$ (Table I). It is noteworthy that about the same number of high-energy protons has been injected into the interplanetary medium soon after the flare, $N^{\text{IPM}}(> 600\,\text{MeV}) = 5.5 \times 10^{30}$ (for the *prompt* component of interplanetary protons by Torsti *et al.*, 1996). The injection spectrum of interplanetary protons was approximated by the function

$$N(E) = N_1 \left(\frac{E_1}{E}\right)^{\gamma_1} \frac{1}{1 + (E/E_2)^{\gamma_2}}. \tag{4}$$

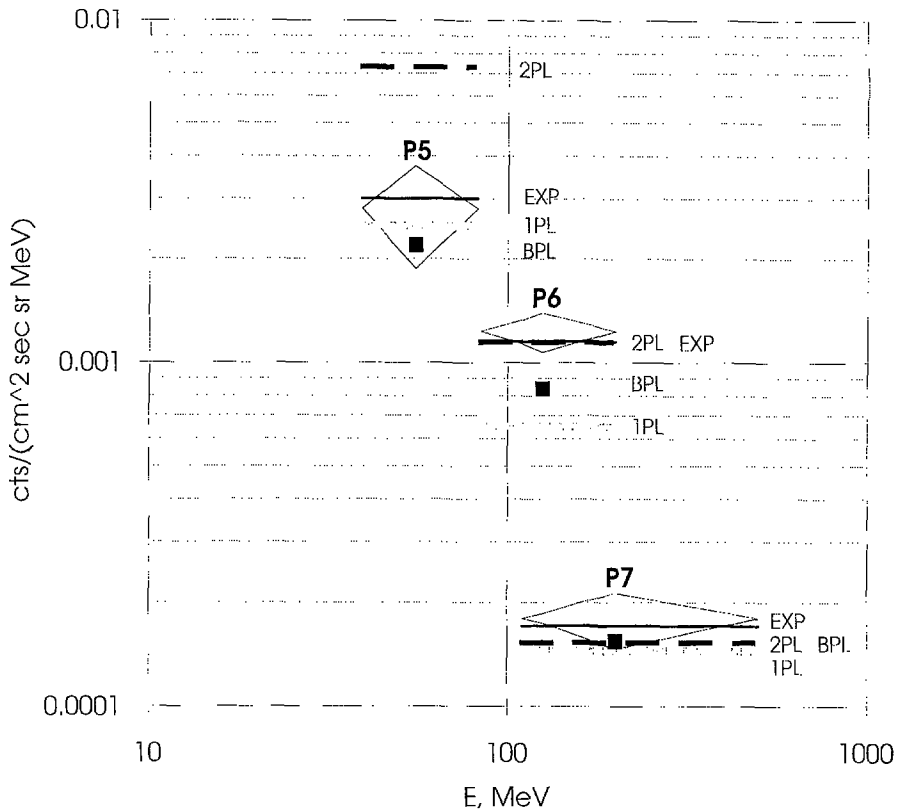

Figure 10. Composite plot of the expected and observed fluxes of neutron-decay protons in three GOES channels. Rhombus-type figures represent the uncorrected averaged counting rates observed on board GOES 6 and 7 during 21:00–21:05 UT (P6 and P7) and 21:05–21:10 UT (P5) on May 24, 1990. Horizontal bars illustrate the expected counting rates for the cases listed in Table II.

where $N_1 = 1.4 \times 10^{30}$ proton MeV^{-1}, $\gamma_1 = 1.6$, $\gamma_2 = 3.0$, $E_1 = 160$ MeV, and $E_2 = 360$ MeV. At high energies ($\approx$1 GeV), this spectrum is close to the spectrum of the s-component of interacting protons, $E^{-4.5}$ (the 2PL-case in Table II). Furthermore, it is seen from Figure 10 that the P5-channel counting rate as expected in the 2PL-case exceeds significantly the observed one. This implies a flattening of the interacting proton spectrum below $\approx$250 MeV. Thus, the s-component spectrum is qualitatively similar to the spectrum of interplanetary protons (4).

As the next step, we adopt spectrum (4) as a possible spectrum of the s-component of interacting protons. The calculated spectrum of solar neutrons produced by protons with spectrum (4) is shown in Figure 11 (marked with BPL). Then we use the BPL neutron spectrum for a fitting of the neutron monitor counting rate. The 90% confidence contour obtained is shown in Figure 12. Marked with BPL is the point sampled for calculations of neutron-decay protons. The corresponding normalisation and other parameters of interacting proton spectra are listed

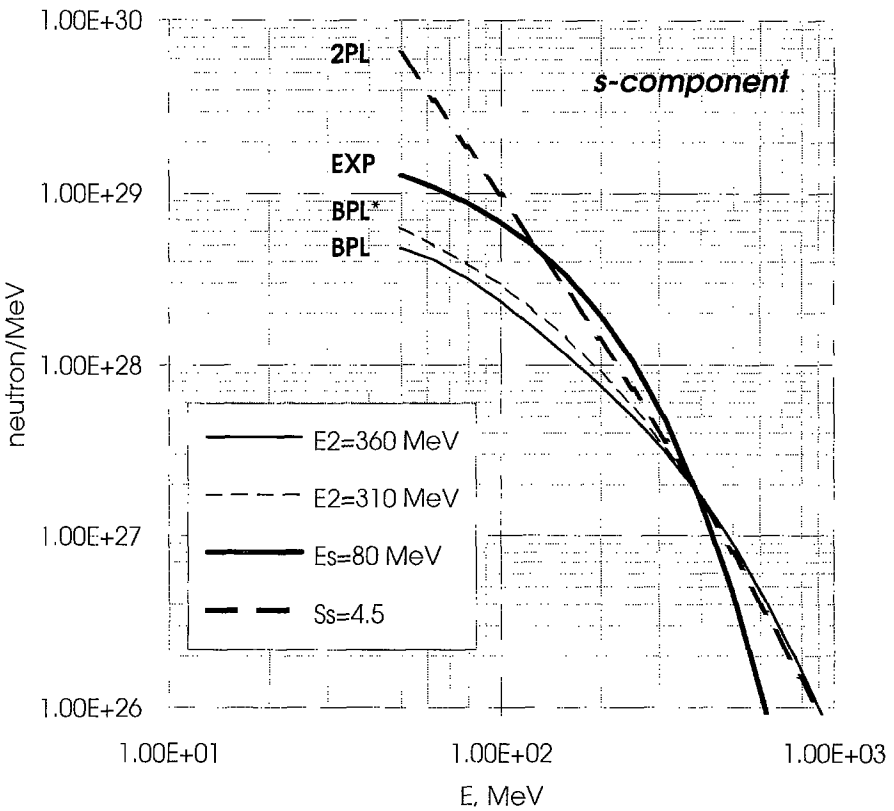

Figure 11. Calculated spectra of the second component of neutrons. Spectra BPL* and EXP fit the data at isotropic ($A_\Delta = 1$) and anisotropic ($A_\Delta = 2$) neutron production, respectively. The parameters of the 2PL, EXP and BPL cases are listed in Table II. In cases BPL and BPL*, the spectrum of interacting protons was taken according to Equation (4) at $E_2 = 360$ MeV and $E_2 = 310$ MeV, respectively.

in Table II. The results of calculations of neutron-decay protons are presented in Figures 7, 8, and 10. It is seen from Figure 10 that, in a comparison with $F(S)$-type neutron spectra, the BPL spectrum fits the P6–P7 channels counting rates better. However, the BPL neutron spectrum still underestimates the P6 channel counting rate (Figure 10).

7. Discussion

7.1. Spectrum of High-Energy Neutrons and Interacting Protons

Two components of neutron injection as well as exponential neutron spectra have been employed by Kovaltsov *et al.* (1994) and Kocharov *et al.* (1994a) for the fitting of the neutron increase observed by neutron monitors on 1990 May 24. In the case

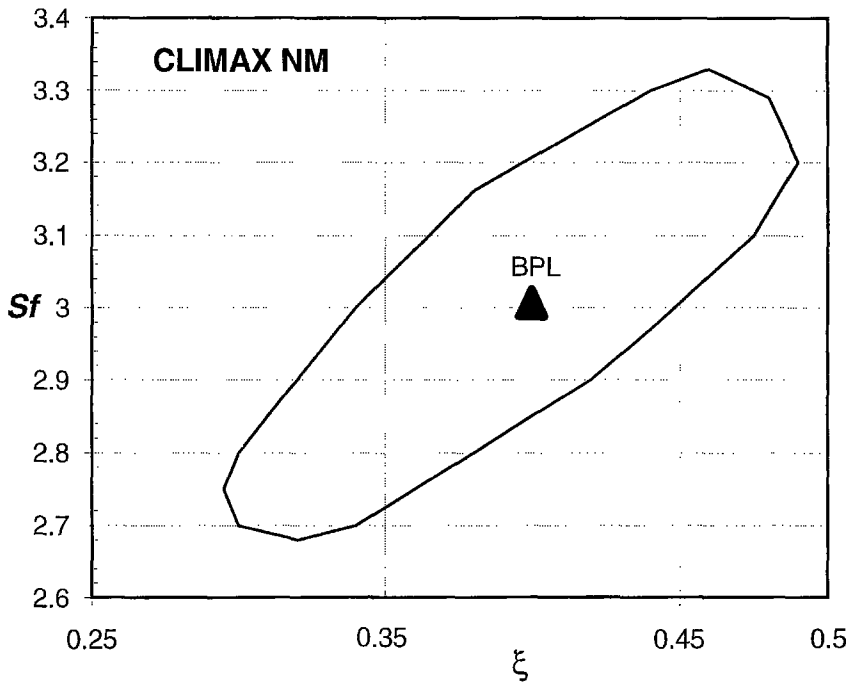

Figure 12. The results of the parameter fitting of the Climax neutron monitor counting rate. The contour represents the 90% confidence level in the (S_f, ξ) plane. The spectrum of the s-component of protons was taken according to Equation (4) at $E_2 = 360$ MeV. The black triangle (BPL) shows the values of parameters sampled for calculations of neutron-decay protons.

of this exponential model, the predicted intensity–time profiles of neutron-decay protons coincide with the GOES observations in the high-energy proton channels. As is the case in physics research, such a coincidence supports the model proposed earlier.

The new analysis of neutron monitor data has been performed with the employment of neutron spectra which are produced by protons with a power-law spectrum in energy. After that, expected fluxes of neutron-decay protons have been compared with the observations. It is seen from the observations in the P6 and P7 channels that, between 150 and 500 MeV, the neutron spectrum is as steep as the spectrum $F(S \approx 4.5)$ (Figure 10). Hence, based on the analysis of neutron monitor data, we conclude that an additional hard component of neutrons was produced in the flare (Figure 5). This component was responsible for the fast increase of neutron monitor counting rate in the beginning of the event (Figure 4). Thus, two populations of neutrons are necessary to explain both neutron monitor and GOES observations.

It is seen from Figure 10 that the intensity of neutron-decay protons as expected in the frame of the two-component model with a soft power-law spectrum of the *second* component of interacting protons (2PL) exceeds the counting rate observed in the GOES P5 channel which implies a flattening of the s-component

neutron spectrum in the energy band below 100–150 MeV. On the other hand, the intensity–time profile of neutron-decay protons as predicted in the frame of the two-component exponential (EXP) model of neutron injection (Kovaltsov *et al.*, 1994; Kocharov *et al.*, 1994a) is in agreement with the proton profiles observed on board GOES. This implies that, in the 50–500 MeV range, the spectrum of solar neutrons was close to an exponent in energy. This neutron spectrum may be prolonged to a band of higher energies either as a power-law proton originated, $F(S)$, or as an exponent in energy, $\exp(-E/E_0)$. There is no experimental device to distinguish these two possibilities. However, a power-law proton originated spectrum of the f-component can not be extended to a band above 2 GeV. The spectrum of neutrons of low energies, <50 MeV, is beyond the scope of the present study.

In an attempt to obtain flattening of the neutron spectrum at low energies, the spectrum of s-component interacting protons has been proposed to be equal to the spectrum of the *prompt* component of interplanetary protons. In this case the number of neutrons with energy 100–200 MeV appeared to be not enough, yet, to obtain good agreement with the intensity of the precursor observed in the GOES P6 channel (see BPL point in Figure 10). Thus, better agreement can be obtained when, in the energy band 200–400 MeV, the spectrum of s-component protons is slightly steeper than the spectrum of interplanetary protons. For this reason, we adopt the spectrum (4) at $E_2 = 310$ MeV to calculate neutron production for the s-component (see Figure 13). It is seen from Figure 11 that, in the case of this spectrum (marked with BPL*), the number of ~100 MeV neutrons is sufficient to fit well the GOES P6 channel counting rate. Thus, it is most likely that the spectrum of s-component protons at ~300 MeV was slightly steeper that the spectrum of *prompt* protons in the interplanetary medium. It is less likely, but still can not be ruled out that both the spectra simply coincided. It is possible that the *second* component of interacting protons and the *prompt* component of protons in the interplanetary medium were two portions of a unitary proton population accelerated during 1–2 min in the impulsive phase of the flare and then trapped for 4–40 min in high magnetic loops in the solar corona. Some re-acceleration during the trapping might produce a hardening of the *prompt* component spectrum before the injection into the interplanetary medium.

It is interesting to compare the results obtained with the observations of neutrons and neutron-decay protons from the famous 1982 June 3 flare (Chupp *et al.*, 1987; Evenson, Kroeger, and Meyer, 1985). It is seen from the composite plot in Figure 8 of Chupp *et al.* (1987) that, in the case of the 1982 June 3 flare, some flattening of the neutron spectrum below 150 MeV may be seen. However the accuracy of reconstruction of the neutron spectrum in the entire 50–500 MeV energy range is not better than 30%. Recent calculations by Ruffolo (1991) support these conclusions. It is important that Ruffolo (1991) made use of better proton data and an updated interplanetary transport model. In the 26–147 MeV range, he approximated the neutron spectrum to be a power law in energy with the neutron

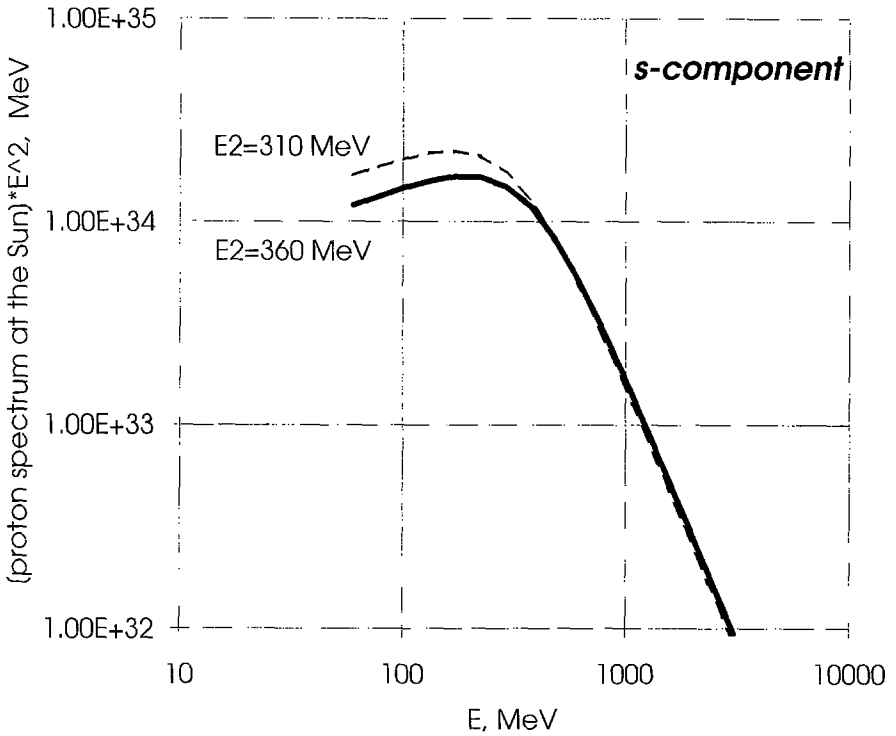

Figure 13. Spectra of interacting protons, multiplied by E_2, used for the calculations of BPL and BPL' neutron spectra shown in Figure 11.

spectrum index $S_n = 1.7-1.9$, while Chupp *et al.* (1987) deduced the value of $S_n = 2.4$ in the energy band 100–2000 MeV. In the case of the 1990 May 24 flare, we make use of an updated transport code. However, only two GOES energy channels in the range of lower energies can be analysed. For this reason, we cannot exclude the possibility that a power-law approximation of the neutron spectrum in the 50–150 MeV range may be better then the exponential one, but such a spectrum definitely cannot be extended to higher energies. Probably, an exponent is not the best approximation of the actual neutron spectrum, but what we conclude is that, in the case of the s-component of neutron emission, the average behaviour of the neutron spectrum can be adequately described with an exponential law in the entire 50–500 MeV energy range. Another possible approximation is the spectrum of neutrons originating from protons with the spectrum (4) at $E_2 = 310$ MeV. One can see from Figure 11 that the accuracy of the exponential approximation is about 30% in the entire 50–400 MeV range, in any case. However, the actual neutron spectrum may be essentially harder than the exponential one at higher energies.

As an alternative to the two-component model with a soft spectrum of the s-component, a model with spectra of both the components being equal to each other has been considered. $S_f = S_s = S$. Such a single population model requires hard

neutron spectra, $F(S < 3.4)$. However, in this case, the maximum possible flux of neutron-decay protons is not sufficient to explain the GOES observations in the P6-channel. Moreover, if $S < 2.5$ it is also impossible to fit the observed P7 channel counting rate. Note that, for $S < 2$, the expected flux of neutron-capture 2.2 MeV gamma-ray line emission, as estimated according to calculations of Hua and Lingenfelter (1987) and Ramaty *et al.* (1993), is about an order of magnitude less than the one reported by Terekhov *et al.* (1993) for the PHEBUS/GRANAT observations. The boundary case of the only s-component existing ($\xi = 0$) requires as hard a spectrum as $F(S = 1.6)$, which implies all the above-mentioned difficulties. Thus, we conclude that the probability of the single population scenario is small.

Let us consider additionally another boundary case of $\xi = 1$, when only the f-component exists (an impulsive neutron production). In this case, none of the $F(S)$ spectra can fit the neutron monitor data. However, in the case of an impulsive neutron production, a time-of-flight approach is possible to deduce the neutron injection spectrum. The neutron spectrum deduced by such a means is close to $F(S = 3.5)$ in the band of 300 – 1500 MeV, while it turns out to be much softer at lower energies. This fact may be considered again as a signature of two interacting proton components. However, the spectral index of the soft component protons becomes extremely high when ξ approaches 1 (see, e.g., Table I). Note that the case of $\xi \approx 1$ has no support in observations of electromagnetic emissions of the flare.

7.2. Possibility of the Third Neutron Injection

We studied a possible impact of a hypothetically extremely prolonged *third* component of neutron production, which may have no clearly signature in gamma-ray emissions due to a low intensity. Such a component may exist because the injection of the *prompt* component of protons into the interplanetary medium had the e-folding time of 40 min (Torsti *et al.*, 1996). No one can exclude the possibility that some portion of the protons simultaneously precipitated into the chromosphere to produce the third component of high-energy neutrons with the e-folding time 2400 s, as well. Debrunner, Lockwood, and Ryan (1993) proposed to use Mexico City neutron monitor data for extrapolation of the Climax neutron monitor counting rate after 21:03 UT on May 24, 1990. This approach showed (Debrunner, Lockwood, and Ryan, 1993; Kovaltsov *et al.*, 1995) that some very prolonged neutron emission from the Sun might exist for the event. However, this interpretation of the Mexico City monitor counting rate recorded after 21:05 UT cannot be proved for sure because of the possible impact of solar protons. For this reason, we can use the counting rate observed after 21:05 UT to put an upper limit for the *third* component of high-energy neutron production, only. By means of fitting of the Mexico City counting rate, the upper limit for the total number of the third component of interacting protons may be obtained as $N^{(3)}_{\max}(> 600 \text{ MeV}) = 3 \times 10^{30}$ (the BPL

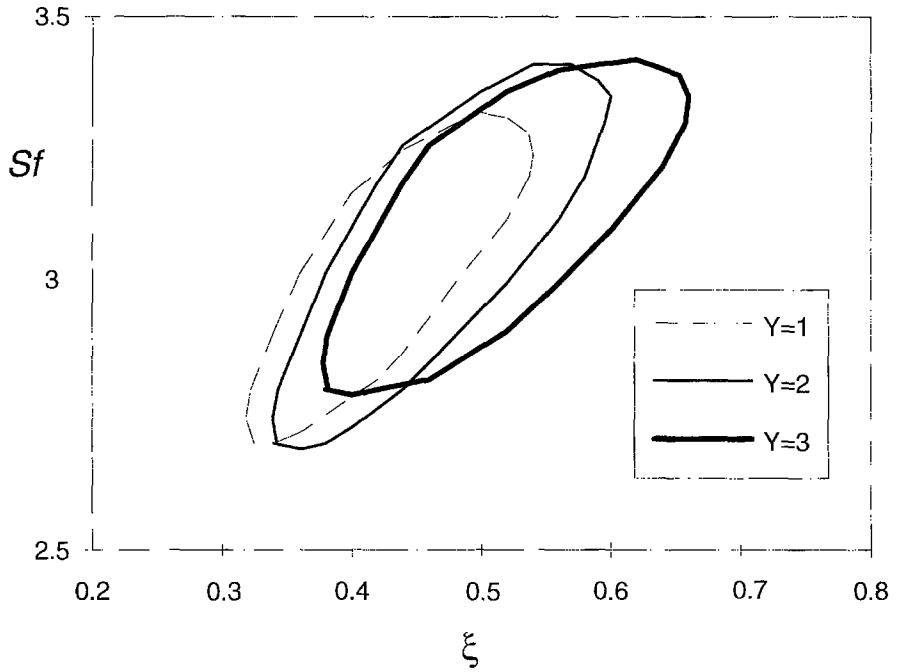

Figure 14. The results of the parameter fitting of the Climax neutron monitor counting rate in the case of the third component introduced, for different values of the parameter Y (see text). The contours represents the 90% confidence levels in the (S_f, ξ) plane. For both the second and third components of neutrons, the BPL spectrum was used.

neutron spectrum is used for the third neutron component). In order to calculate the contribution of the third component into the neutron monitor counting rate, we introduced the parameter $Y \equiv N^{(3)}(> 600 \text{ MeV})/10^{30}$. The Climax neutron monitor counting rate has been fitted at different values of the parameter $Y \in [0, 3]$. In Figure 14 we show the 90% confidence contours obtained. Some best-fit parameters are presented in Table I. It is seen from Figure 14 that the introduction of the third component of high-energy neutrons results mainly in a shift of the values of the parameter ξ. Thus, a possible contribution of the *third* component neutron is not very essential for the analysis.

The *third* component being introduced does not change essentially the flux of neutron-decay protons during the time when the 'precursor' can be observed. As an example, Figure 9 shows the intensity–time profile of neutron-decay protons for the case of $Y = 1.0, \xi = 0.4, S_f = S_s = 3.0$, and the spectrum of third-component neutrons taken as $F(S = 4.5)$ (this case is marked with 3PLA in the figure and in Table II). For a comparison, the 1PLA case ($Y = 0$) is shown as well.

7.3. INTERPLANETARY-TO-INTERACTING PARTICLE RATIO

In a high-energy band, the ratio of interplanetary to interacting particles is a subject of large uncertainties, because every high-energy secondary emission may be anisotropic. Nevertheless, we are interested in this ratio because, being calculated under the certain 'standard' propositions for different flares, it may reveal the dependence on a flare type, position on the solar disc, etc. We calculated this ratio under the proposition of isotropic production of neutrons, which may be the case if the flare is situated near the solar limb and/or the magnetic field at the flare site is tilted and sufficiently complicated. Being calculated under this proposition, the interplanetary-to-interacting proton ratio $N^{\mathrm{IPM}}(> 600\ \mathrm{MeV})/N_0(> 600\ \mathrm{MeV}) = 1-2$ (Table I and Torsti *et al.*, 1996). In the case of anisotropic neutron production, the total number of >600 MeV interacting protons should be renormalised as $N_0(> 600\ \mathrm{MeV}) \rightarrow N_0(> 600\ \mathrm{MeV})A$, where A is the anisotropy factor defined as the ratio of the angle averaged number of high-energy neutrons at the Sun to the number of neutrons emitted towards the Earth. One can expect the anisotropy factor $0.5 < A < 3$ for a near-limb flare (e.g., Kocharov *et al.*, 1995). Note that the expected number of secondary neutrons depends also on the composition of accelerated particles and that of ambient plasma (Ramaty *et al.*, 1993). This implies that, in the case of a composition enriched with He, the total number of interacting protons may be 2--3 times less than the number deduced under the standard composition by Hua and Lingenfelter (1987), which was actually used in the present paper. Anyway, the total number of interplanetary protons is not less than 30% of the total number of protons interacting at the Sun (cf., Debrunner, Lockwood, and Ryan, 1993). Note that, for the flare of 1982 June 3, Ramaty *et al.* (1993) obtained the ratio of interplanetary to interacting >30 MeV protons to be 0.26–1.3, depending on the composition of the particles.

8. Conclusions

The main results of this study are the following:

(1) The high magnitude of the 1990 May 24 neutron event provided an opportunity to study the flux of neutron-decay protons of higher energies than ever before. A 'precursor' was clearly seen in the high-energy proton channels of the GOES detectors before the onset of the major proton event. This 'precursor' can be explained naturally as originating from decay of solar neutrons in the interplanetary medium.

(2) The observed counting rate of the Climax neutron monitor may be fitted under two assumptions: (i) a single population of interacting protons with a hard power-law spectrum ($S_f - S_s \leq 3.4$); (ii) two proton components with a hard spectrum component generating neutrons during a short time and a longer interacting soft component.

(3) Single population models with hard power-law proton spectra imply a flux of neutron-decay protons which is essentially less than the intensity of the precursor observed in the GOES P6 channel.

(4) The intensity – time profile of neutron-decay protons expected in the frame of the two-component model with a soft power-law spectrum of the second component ($S_s = 4.5$) coincides with the GOES observations in the P6 and P7 channels. This supports the idea of a soft spectrum of s-component protons. Such a soft spectrum of the s-component implies a hard spectrum of the first component, since this is necessary for the fitting of the observed neutron monitor counting rate.

(5) The likelihood of the two-component model is found to be significantly higher than that of the single population model.

(6) The intensity of neutron-decay protons as expected in the frame of the two-component model with a soft power-law spectrum of the *second* component of interacting protons ($S_s = 4.5$) exceeds significantly the counting rate observed in the GOES P5 channel, which implies a flattening of the neutron spectrum in the energy band below 100 – 150 MeV. The intensity – time profile of neutron decay protons expected in the frame of the two-component exponential model of neutron injection (Kocharov *et al.*, 1994a) is in agreement with the proton profiles observed in all GOES channels. Hence, in the entire 50 – 500 MeV range, the average behaviour of the second component neutron spectrum followed the exponential law in energy.

(7) The spectrum of the second component of interacting protons was qualitatively similar and close to the injection spectrum of the *prompt* component of interplanetary protons at high energies, $E = 100 - 1000$ MeV. It is most likely that the spectrum of interacting protons was slightly steeper at ~300 MeV than the spectrum of interplanetary protons. However, we cannot rule out that both spectra did just coincide.

(8) The total number of interacting >600 MeV protons is found to be of the order of magnitude of the total number of the *prompt* component protons injected into the interplanetary medium.

Acknowledgements

We thank the Academy of Finland for financial support. One of us (GAK) was supported at A. F. Ioffe Physical-Technical Institute by the International Science Foundation and the Russian Government (grant J56100).

References

CD GOES: 1992, *Space Environment Monitor 1-Minute and 5-Minute Averages, January 1986 – June 1992*, Version 1, National Geophys. Data Center, 325 Broadway, Boulder, CO, U.S.A.

Chupp, E. L., Debrunner, H., Flückiger, E., Forrest, D. J., Golliez, F., Kanbach, G., Vestrand, W. T., Cooper, J., and Share, G.: 1987, *Astrophys. J.* **318**, 913.

Chupp, E. L.: 1990, *Astrophys. J. Suppl. Ser.* **73**, 213.
Debrunner, H., Lockwood, J. A., and Ryan, J. M.: 1993, *Astrophys. J.* **409**, 822.
Evenson, P., Meyer, P., and Pyle, K. R.: 1983, *Astrophys. J.* **274**, 875.
Evenson, P., Kroeger, R., and Meyer, P.: 1985, *Proc. 19th Int. Cosmic Ray Conf., La Jolla* **4**, 130.
Evenson, P., Kroeger, R., Meyer, P., and Müller, D.: 1983, *Proc. 18th Int. Cosmic Ray Conf.* **4**, 97.
Evenson, P., Kroeger, R., Meyer, P., and Reames, D.: 1990, *Astrophys. J. Suppl.* **73**, 273.
Gueglenko, V. G., Kocharov, G. E., Kovaltsov, G. A., Kocharov, L. G., and Mandzhavidze, N. Z.: 1990, *Solar Phys.* **125**, 91.
Guglenko, V. G., Efimov, Yu. E., Kocharov, G. E., Kovaltsov, G. A., Mandzhavidze, N. Z., Terekhov, M. M., and Kocharov, L. G.: 1990, *Astrophys. J. Suppl.* **73**, 209.
Hua, X.-M. and Lingenfelter, R. E.: 1987, *Solar Phys.* **107**, 351.
Kocharov, G. E., Kocharov, L. G., Kovaltsov, G. A., Shea, M. A., Smart, D. F., Armstrong, T. P., Pyle, K. R., and Chuikin, E. L.: 1993, *Proc. 23rd Int. Cosmic Ray Conf.* **3**, 107.
Kocharov, L. G., Lee, J. W., Zirin, H., Kovaltsov, G. A, Usoskin, I. G., Pyle, K. R., Shea, M. A., and Smart, D. F.: 1994a, *Solar Phys.* **155**, 149.
Kocharov, L. G., Kovaltsov, G. A, Kocharov, G. E., Chuikin, E. L., Usoskin, I. G., Shea, M. A., Smart, D. F., Melnikov, V. F., Podstrigach, T. S., Armstrong, T. P., and Zirin, H.: 1994b, *Solar Phys.* **150**, 267.
Kocharov, L. G., Lee, J. W., Wang, H., Zirin, H., Kovaltsov, G. A, and Usoskin, I. G.: 1995, *Solar Phys.* **158**, 95.
Kocharov, L., Kovaltsov, G., Torsti, J., Usoskin, I., Zirin, H., Anttila, A., and Vainio, R.: 1996, in R. Ramaty, N. Mandzhavidze, and X. M. Hua (eds.), *Proc. High Energy Solar Physics Workshop*, American Institute of Physics, Vol. 374, p. 246.
Kovaltsov, G. A., Efimov, Yu. E., and Kocharov, L. G.: 1993, *Solar Phys.* **144**, 195.
Kovaltsov, G. A., Kocharov, G. E., Kocharov, L. G., and Usoskin, I. G.: 1994, *Astron. Letters* **20**, No. 5, 658.
Kovaltsov, G. A., Kocharov, L. G., Usoskin, I. G., Kananen, H., and Tanskanen, P.: 1995, *Proc. 24th Int. Cosmic Ray Conf.* **4**, 155.
Kurganov, I. G. and Ostryakov, V. M.: 1989, *Izvestia Acad. Nauk SSSR, Ser. Fiz.* **52**, 381.
Kurganov, I. G. and Ostryakov, V. M.: 1992, *Geomagn. i Aeron.* **32**, 149.
Lee, J. W., Gary, D. E., and Zirin, H.: 1994, *Solar Phys.* **152**, 409.
Pelaez, F., Mandrou, P., Niel, M., Mena, B., Vilmer, N., Trottet, G., Lebrun, F., Paul, J., Terekhov, O., Sunyaev, R., Churazov, E., Gilfanov, M., Denisov, D., Kuznetsov, A., Dyachkov, A., and Khavenson, N.: 1992, *Solar Phys.* **140**, 121.
Pyle, K. R., Shea, M. A., and Smart, D. F.: 1991, *Proc. 22nd Int. Cosmic Ray Conf.* **3**, 57.
Ramaty, R., Mandzhavidze, N., Kozlovsky, B., and Skibo, J. G.: 1993, *Adv. Space. Res.* **13**(9), 275.
Ruffolo, D.: 1991, *Astrophys. J.* **382**, 688.
Shea, M. A., Smart, D. F., and Pyle, K. R.: 1991, *Geophys. Res. Letters* **18**, 1655.
Talon, R., Trottet, G., Vilmer, N., Barat, C., Dezalay, J.-P., Sunyaev, R., Terekhov, O., and Kuznetsov, A.: 1993, *Solar Phys.* **147**, 137.
Terekhov, O., Sunyaev, R., Kuznetsov, A., Barat, C., Talon, R., Trottet, G., and Vilmer, N.: 1993, *Pis'ma v Astron. Zh. (Astron. Letters)* **19**, No. 3, 163.
Trottet, G.: 1994, in J. M. Ryan and W. T. Vestrand (eds.), *American Institute of Physics Conf. Proc.* **294**, 3.
Torsti, J., Kocharov, L. G., Vainio, R., Anttila, A., and Kovaltsov, G. A.: 1996, *Solar Phys.* **166**, 135.
Vilmer, N.: 1994, *Astrophys. J. Suppl.* **90**, 611.
Zhang, L. D.: 1995, *Astrophys. J.* **449**, 386.